

A Penta-Band Printed Monopole Antenna for MIMO Applications

Sajad Mohammad-Ali-Nezhad^{1, *} and Hamid R. Hassani²

Abstract—An E-shaped printed monopole antenna with loaded resonant elements suitable for penta-band multi-input multi-output (MIMO) application is proposed. The simple E-shaped monopole antenna results in a single resonance, and by loading the vertical arm of the antenna with narrow slots and stubs, a multi-band antenna can be obtained. The slots so placed on the antenna create L-shaped resonance paths which are multiples of $\lambda_g/4$, and stubs resonate at $\lambda_g/4$. The antenna is designed for operation over the UMTS, WiMAX and WLAN frequencies 2.1, 2.5, 3.5, 5.2, 5.8 GHz. A two element array of such antennas with close spacing of $\lambda_g/15$ is suitable for MIMO application. The array has low mutual coupling, low envelope correlation, high efficiency and good radiation patterns over all five frequency bands. Simulation and measurement results are compared and discussed.

1. INTRODUCTION

To improve the characteristics of wireless communication systems, multiple-input multiple-output (MIMO) systems are employed. These systems are made up of several input and output elements so as to increase the capacity and decrease the multipath fading as compared with single-input single-output (SISO) systems. The factors influencing the increase in channel capacity in MIMO systems are high gain, wide lobe pattern, low mutual coupling, polarization diversity and pattern diversity [1–4].

One of the key elements in MIMO systems is the antenna structure. Although there is extensive literature on non-printed MIMO antennas such as Planar inverted F antennas (PIFA) [5], dielectric resonator antenna [6] and magneto-electric dipole antennas [7], the printed antennas are strongly favored due to their low price, straightforward manufacture, and the capability of easily being integrated to small terminal devices. The design of a dual-element patch microstrip MIMO antenna with high isolation is reported in [8]. In [9], a dual-band microstrip patch MIMO antenna is reported.

Among printed antennas, printed monopole antenna due to its omnidirectional pattern is more appropriate for MIMO application, as this feature enhances the channel capacity [1] while receiving the entirety of multi-path signals. The design of a single band four-element printed monopole antenna for LTE base station application is given in [10]. In [11], a low profile printed MIMO antenna with split ring resonators for WLAN applications is presented.

Recently, there has been an increase in the use of MIMO antennas operating at several frequency bands in wireless communication systems. Among these bands one can refer to UMTS (1.92–2.17 GHz), WiMAX (2.3–2.4, 2.5–2.69 and 3.4–3.6 GHz) and WLAN (2.4–2.48, 5.15–5.35 and 5.725–5.875 GHz). In [12], a dual-band MIMO antenna composed of two closely arranged symmetric monopole antennas with edge-to-edge distance of 5.3 mm is presented for WLAN applications. A tri-band E-shaped printed monopole antenna loaded with two U-shaped resonance paths of $\lambda_g/4$ suitable for MIMO system operating at 2.4, 5.2 and 5.8 GHz is reported in [13]. In [14], a triple-band C-shaped printed monopole antenna for MIMO application covered 2.1–2.6, 3.3–4, and 5.4–6 GHz is reported. A Compact Triband

Received 4 May 2018, Accepted 9 June 2018, Scheduled 22 June 2018

* Corresponding author: Sajad Mohammad-Ali-Nezhad (s.mohammadalinezhad@qom.ac.ir).

¹ Electrical & Electronics Engineering Department, University of Qom, Qom, Iran. ² Electrical & Electronics Engineering Department, Shahed University, Tehran, Iran.

Quad-Element MIMO Antenna Using SRR Ring for High Isolation is reported in [15]. A quad-band F-shaped printed slot antenna for WLAN and WiMAX MIMO system is reported in [16]. In [17], a quad-band MIMO antenna employing split-ring resonator and inter-digital capacitor operating at 1.95, 2.39, 2.64 and 3.27 GHz is reported.

In this paper, a penta-band E-shaped printed monopole antenna suitable for MIMO applications is proposed. By introducing resonance paths on the vertical arm of the E-shaped antenna, which is carried out through insertion of slots and stubs, five separate resonance bands can be obtained from the antenna at the frequencies of 2.1, 2.5, 3.5, 5.2 and 5.8 GHz. The various configurations of such antennas in relation to each other are investigated and based on the least correlation, mutual coupling and optimal radiation patterns the most suitable configuration for MIMO application is presented. Simulation results via software package HFSS and measured results are compared and discussed.

2. GENERATION OF RESONANCE FREQUENCIES

The E-shaped printed monopole antenna introduced in [10] has been shown to be suitable for MIMO application. This antenna structure can be further developed to include higher number of frequency bands with tuning capabilities.

The basic structure of the E-shaped printed monopole antenna is shown in Fig. 1(a) having a single resonance within the WLAN frequency range. To increase the number of frequency bands, higher resonance modes should be activated, i.e., more resonance paths should be introduced on the basic E-shaped antenna structure. Such resonance paths which are multiples of $\lambda_g/4$ in length can be created by placing narrow slots on the vertical arm of the E-shaped antenna.

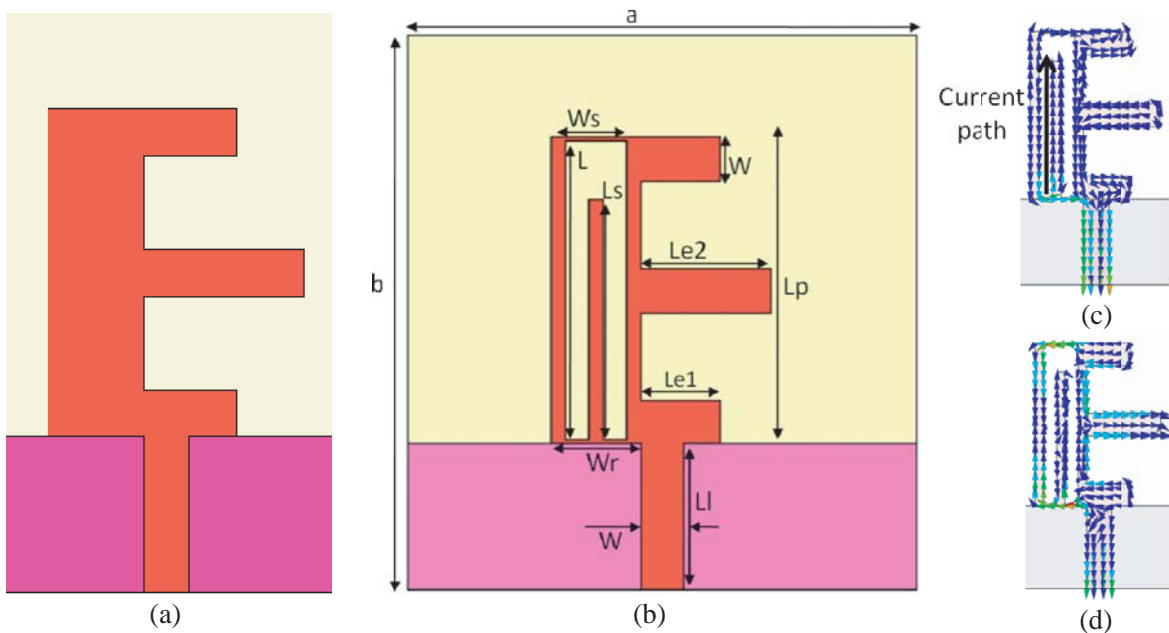


Figure 1. E-shaped monopole antenna, (a) without slot, (b) with slot and stub and surface current distribution on the E-shaped monopole antenna with slot and stub (c) at 3.5 GHz and (d) at 5.8 GHz.

To increase the number of resonant frequencies, one can also add a stub line of $\lambda_g/4$ in length either inside or attached outside to the slot as shown in Fig. 1(b). Figs. 1(c) and (d) show the relevant current distributions at 3.5 and 5.8 GHz. The current distribution on the antenna at 5.8 GHz is shown in Fig. 1(d), where the existence of two current paths (in this case L-shaped one) is conspicuous. The total length of these two current paths is $3\lambda_g/4$. By splitting the single slot into more slots the number of current paths and hence the number of resonant frequencies can be increased. However, if the paths are too close to each other in length, rather than generating other resonant frequencies a widening of

the frequency band takes place.

Increasing the number of such stubs increases the number of resonance frequencies. If wide bandwidth is required at a particular frequency, several close resonances should be created. This can be done by using several stubs of nearly equal lengths.

To obtain the resonant frequencies the following formula can be used for the length of the L-shaped current paths and for the stubs:

$$2 * W_s + L \cong 3\lambda_g/4 \tag{1}$$

$$L_s \cong \lambda_g/4 \tag{2}$$

To increase the number of resonant bands, a combination of the above-mentioned techniques can be employed.

3. THE TRI-BAND E-SHAPED PRINTED MONOPOLE ANTENNA

The substrate used for the proposed antenna has a permittivity $\epsilon_r = 4.4$, thickness $h = 0.8$ mm and dimension of $29.5 * 27$ mm². The optimal antenna parameters for the tri-band behavior at 2.4, 3.5 and 5.8 GHz are set as follows: $L_p = 14.75$ mm, $L = 14.35$ mm, $Ll = 8$ mm, $Le1 = 4.1$ mm, $Le2 = 6.75$ mm, $L_s = 12$ mm, $W = 2$ mm, $W_s = 3.1$ mm and $W_r = 4.6$ mm. In order to obtain these parameters at first dimensions were obtained from formulas (1) and (2) based on the resonance frequencies, and then they were optimized in HFSS software.

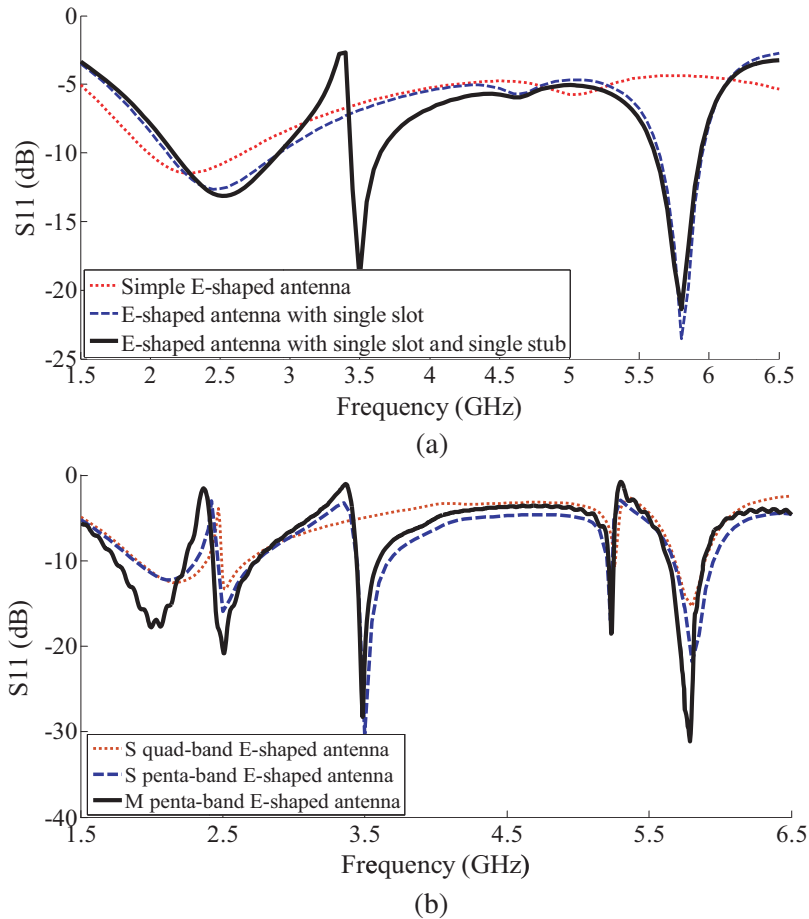


Figure 2. Simulated (S) reflection coefficients of the E-shaped antenna, (a) without slot, with single slot and single slot with a stub, (b) with two slots and single stub and Simulated (S) and Measured (M) reflection coefficient of the E-shaped antenna with two slots and two stubs.

Figure 2 shows the simulated reflection coefficient of the antennas shown in Fig. 1. As can be seen, the simple E-shaped monopole antenna has a resonance frequency at 2.4 GHz. Placement of a single slot on the antenna leads to two L-shaped current paths and creates a resonance at 5.8 GHz while maintaining the initial resonance at 2.4 GHz. This shows that the 2.4 GHz band is independent of the other resonance. Adding a stub to the aforementioned structure gives the structure of Fig. 1(b). Fig. 2 shows that a resonance at 3.5 GHz is established without affecting the previous two resonance frequencies.

4. QUAD AND PENTA-BAND E-SHAPED PRINTED MONOPOLE ANTENNA

The creation of 3 or 4 resonance paths on the vertical arm of the E-shaped antenna can give rise to 4 or 5 resonance frequencies, respectively. Figs. 3(a) and (b) show the structure of the E-shaped printed monopole antenna with combination of slots and stubs to produce quad- and penta-bands. The dimensions of the main E-shaped printed monopole antenna are similar to that of the previous section. The optimized dimensions of the other parameters of the quad-band antenna are $Lp = 17.2$ mm, $Ls1 = 16.25$ mm, $Ls2 = 16.5$ mm, $Ls3 = 12$ mm, $Wr = 3.35$ mm, $Ws1 = 0.55$ mm, $Ws2 = 2.75$ mm and $Ws3 = 1.75$ mm and the dimensions of the other parameters of the penta-band antenna are

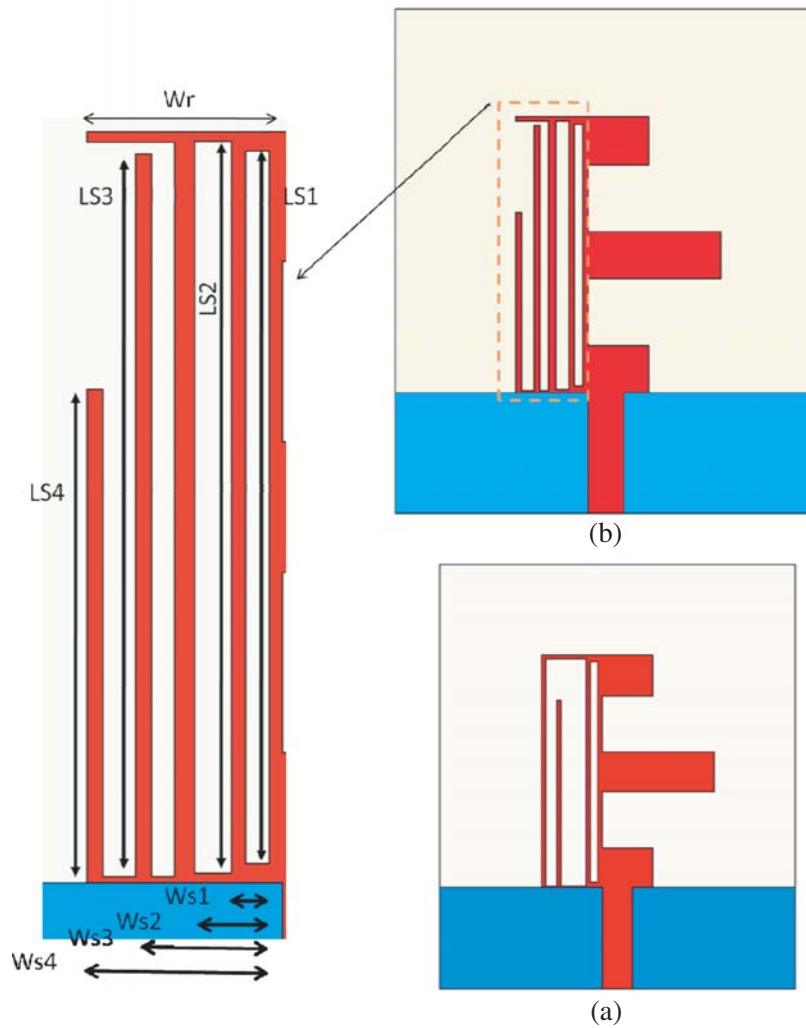


Figure 3. E-shaped monopole antenna, (a) with two slots and single stub, (b) with two slots and two stubs.

$L_p = 17.2$ mm, $L_{s1} = 16.25$ mm, $L_{s2} = 16.7$ mm, $L_{s3} = 16.6$ mm, $L_{s4} = 10.9$ mm, $W_r = 4.5$ mm, $W_{s1} = 0.55$ mm, $W_{s2} = 1.75$ mm, $W_{s3} = 2.7$ mm and $W_{s4} = 3.8$ mm.

Figure 2(b) shows the reflection coefficient of the quad- and penta-band antenna. The simulation results show that the center resonance frequencies of all the bands can be obtained as required. In this procedure, it is noticed that the bandwidth of the 5.2 GHz resonance does not cover the required 5.15–5.35 GHz band. To increase the bandwidth of this band, without affecting the performance of other bands, one can add an additional resonance at 5.3 GHz just beside the existing resonance at 5.2 GHz. This additional resonance is created by inserting an extra U-shaped path very close to the previous U-shaped path for 5.2 GHz.

To increase the bandwidth for this application, the authors have created an additional resonance just beside the existing resonance at 5.2 GHz in 5.3 GHz. This additional resonance is created by inserting an extra U-shaped path very close to the previous U-shaped path for 5.2 GHz. The insertion of this extra U-shaped path does not disturb the results obtained previously for other frequency bands, i.e., its presence is independent of the others. The dimension of this extra path is $W_s = 2.25$ mm and $L_s = 16.7$ mm. Fig. 4 shows modified penta-band E-shaped monopole antenna.

Figure 5 shows the simulated and measured reflection coefficients of the penta-band E-shaped printed monopole antenna along with the shape of the relevant antenna. Table 1 presents the impedance

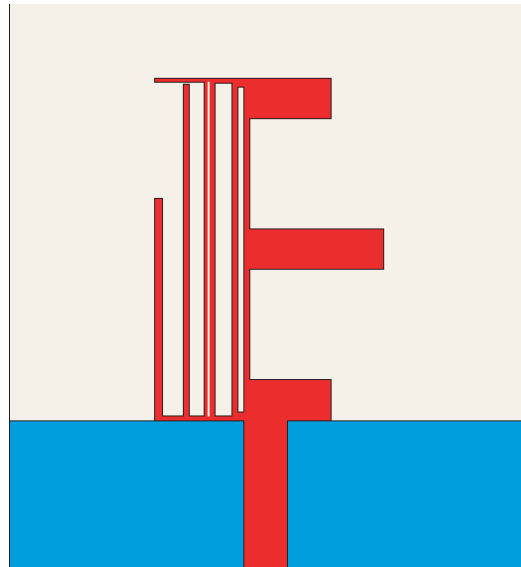


Figure 4. Modified E-shaped printed monopole antenna with three slots and two stubs.

Table 1. Impedance bandwidth of the standard bands along with those of the proposed E-shaped antenna and its modified version.

Impedance bandwidth of Standard Bands (GHz)	UMTS 1.92–2.17	WLAN 2.4–2.48	WiMAX 3.4–3.6	WLAN 5.15–5.35	WLAN 5.725–5.875
Impedance bandwidth of the proposed Penta band antenna (GHz)	1.75–2.2	2.4–2.6	3.4–3.6	5.15–5.25	5.67–5.9
Impedance bandwidth of the Modified antenna (GHz)	1.75–2.2	2.4–2.6	3.4–3.6	5.15–5.35	5.67–5.9

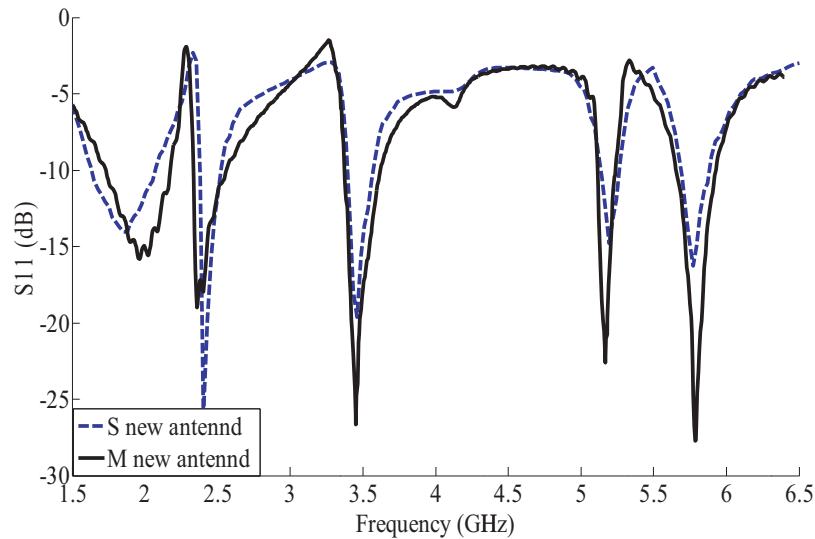


Figure 5. Simulated (S) reflection coefficient of the E-shaped antenna for penta band.

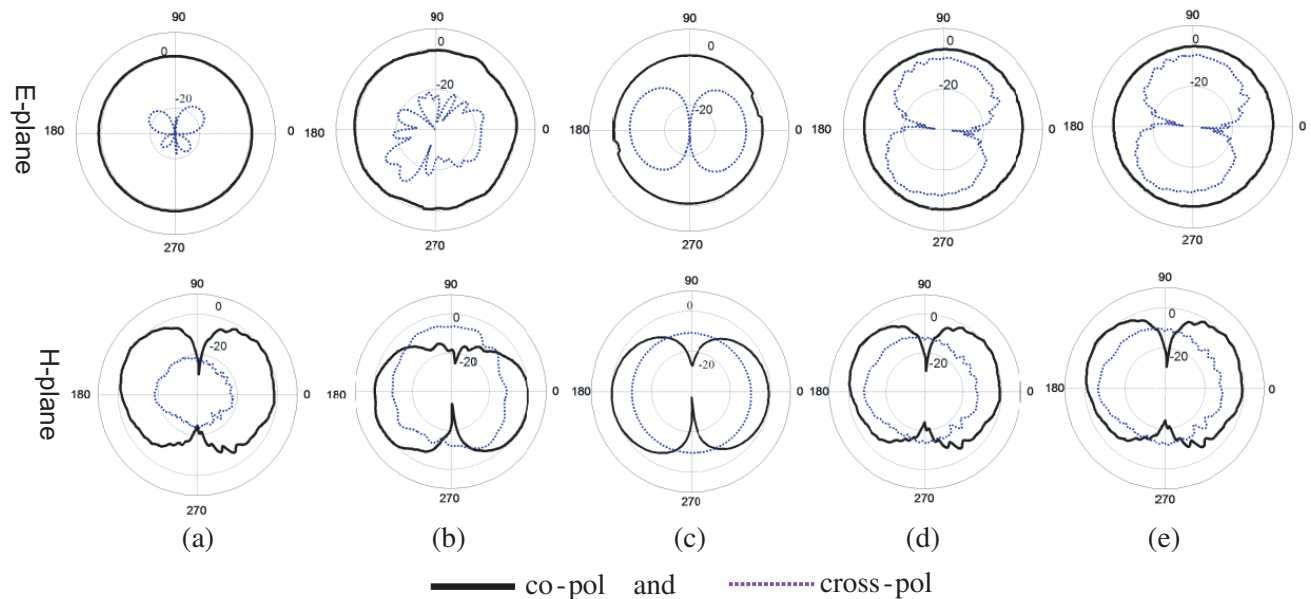


Figure 6. Measured E - and H -plane radiation patterns of the proposed penta-band antenna at (a) 2.1 GHz, (b) 2.5 GHz, (c) 3.5 GHz, (d) 5.2 GHz, (e) 5.8 GHz.

bandwidth of the penta-band antenna structure with and without the implementation of the extra U-path. The standard impedance bandwidth for each application is also shown in this table.

As mentioned before, by placing various slots and stubs of appropriate dimensions in the vertical arm of the E-shaped antenna one can obtain any resonance frequency over the UMTS, WLAN and WiMAX frequency ranges.

Table 2 presents the resonance frequencies of the quad-band antenna along with the relevant dimensions of the slots and stubs. For certain resonance frequencies, one can remove either a slot or a stub from the structure. Also, for penta-band operation, by varying Ls_4 from 11.2 mm to 12.7 mm frequencies from 3.3 GHz to 3.7 GHz can be obtained.

The measured E and H -plane radiation patterns of the new penta-band antenna are shown in Fig. 6. Both the co- and cross-polar components are shown. It is noticed that the antenna has an

Table 2. Various resonance frequencies over UMTS, WLAN and WiMAX range as obtained by optimizing the slots and stubs dimensions.

Resonance frequency (GHz)	$Ws4$ (mm)	$Ls4$ (mm)	$Ws3$ (mm)	$Ls3$ (mm)	$Ws2$ (mm)	$Ls2$ (mm)	$Ws1$ (mm)	$Ls1$ (mm)
2.1, 2.5, 5.2 and 5.8	removed	removed	1.75	16.5	2.75	15.75	0.55	16.25
2.1, 3.3, 5.2 and 5.8	removed	removed	1.75	13	2.75	15.75	0.55	16.25
2.1, 3.5, 5.2 and 5.8	removed	removed	1.75	12	2.75	15.75	0.55	16.25
2.1, 3.7, 5.2 and 5.8	removed	removed	1.75	11	2.75	15.75	0.55	16.25
2.1, 2.5, 3.3 and 5.8	0.75	13	1.75	16.5	2.75	15.75	removed	removed
2.1, 2.5, 3.5 and 5.8	0.75	12	1.75	16.5	2.75	15.75	removed	removed
2.1, 2.5, 3.7 and 5.8	0.75	11.2	1.75	16.5	2.75	15.75	removed	removed

omnidirectional E -plane pattern that varies within ± 1 dB and has lower than -12 dB cross polarization in the E -plane over all the frequency bands. Also, the H -plane pattern is very stable with changes in frequency.

5. PENTA-BAND E-SHAPED MONOPOLE ANTENNA FOR MIMO APPLICATION

The design given above results in an antenna element operating at 2.1, 2.5, 3.5, 5.2 and 5.8 GHz suitable for wireless communication. This antenna element can be arrayed for use in MIMO applications. To be suitable for MIMO application, the antenna array should have good radiation pattern, high radiation efficiency, high peak gain, low envelope correlation, and high isolation between the signal ports. These parameters can be obtained from the S -parameters and the radiation patterns. Reflection coefficient and mutual coupling can be obtained as S_{11} , S_{22} and S_{12} . The envelope correlation ρ_e is determined through the use of the far field [18]. Also the peak antenna gain and radiation efficiency can be obtained from radiation patterns.

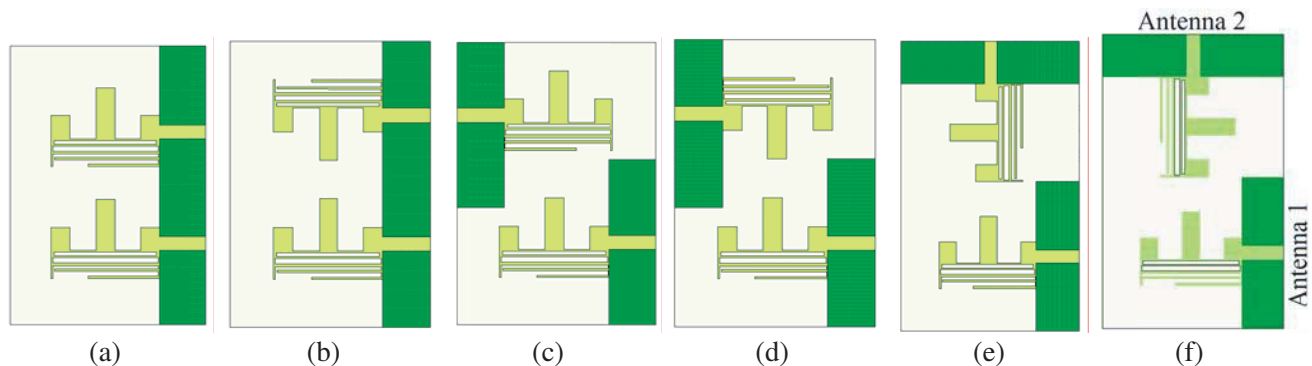
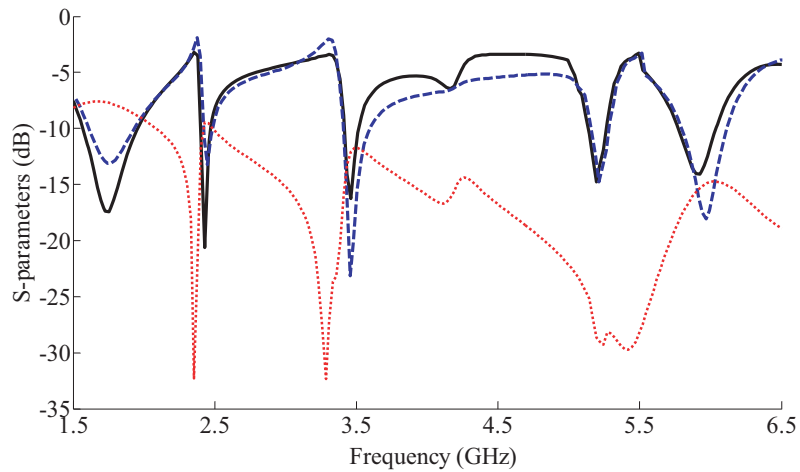
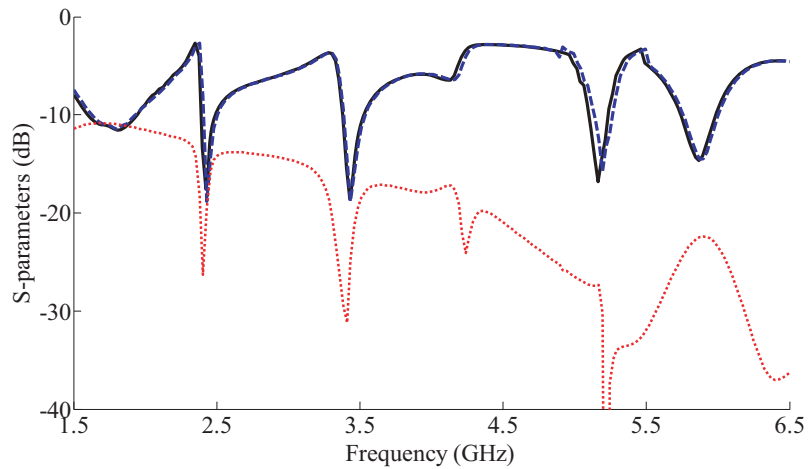


Figure 7. Different configurations of array of two elements of the E-shaped printed monopole antenna with slots and stubs.

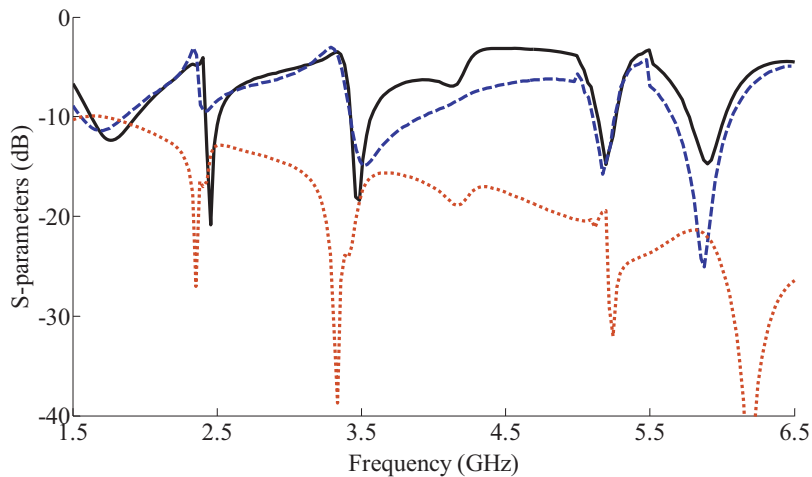
Figure 7 shows six possible configurations of any two E-shaped monopole antennas with their respective grounds. Figs. 8 and 9 show the relevant simulated S -parameters and envelope correlation, respectively. In each case, the spacing between array elements is set at 5.5 mm ($\lambda_g/15$ of the lowest frequency band).



(a)



(b)



(c)

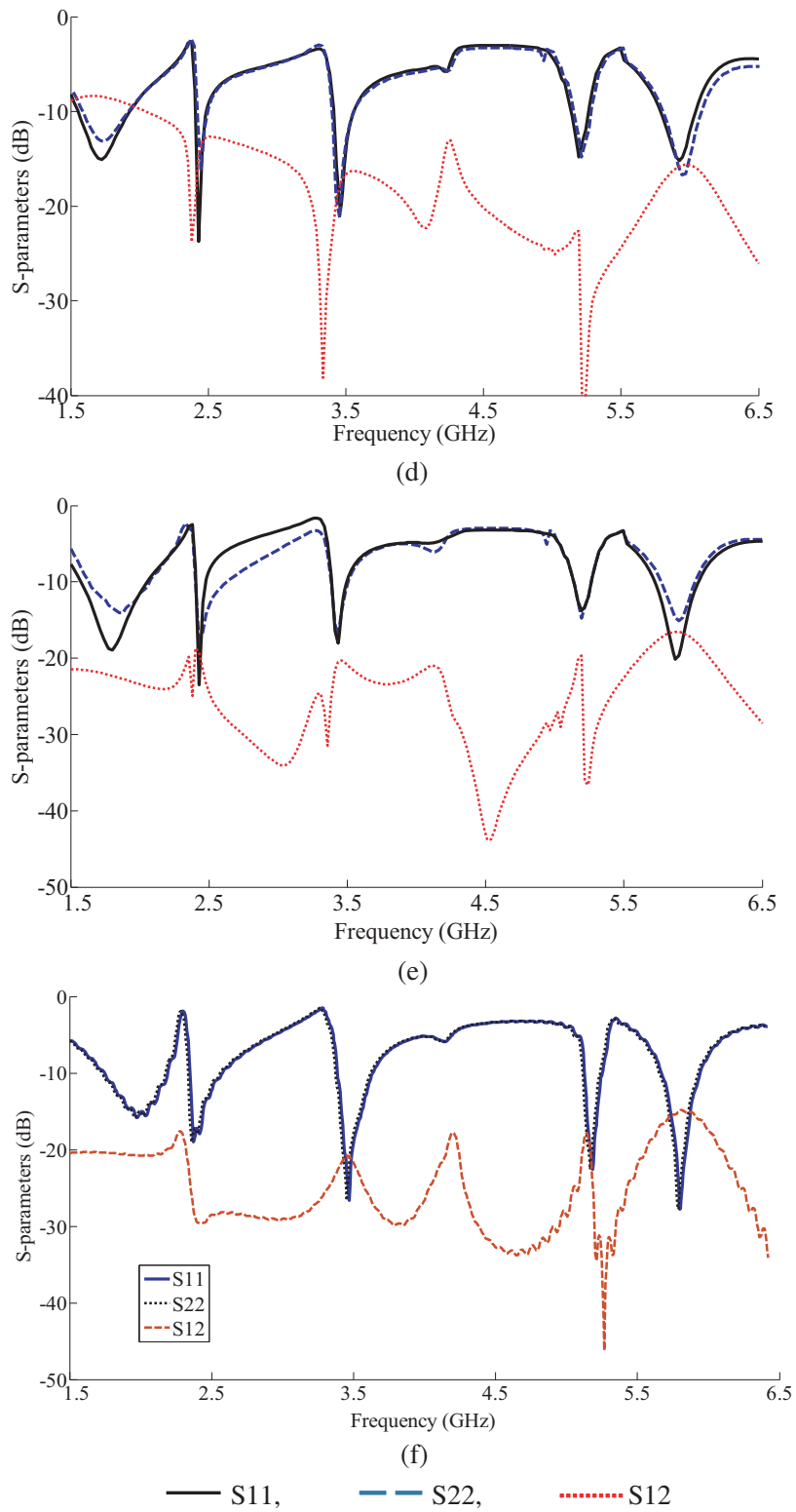


Figure 8. Simulated S -parameters of the MIMO array configuration of structures shown in Fig. 7 and measured proposed configuration of structure f.

Changes in placement of the elements result in different S -parameters and envelope correlation. As can be seen from Figs. 8 and 9, the mutual coupling of the monopole antenna's orthogonal configurations is lower than the mutual coupling of the monopole antenna's parallel configurations. This is because for such orthogonal elements, the radiation pattern and polarization of each element lies on a plane orthogonal to the other, causing stable radiation pattern and less mutual coupling and envelope correlation.

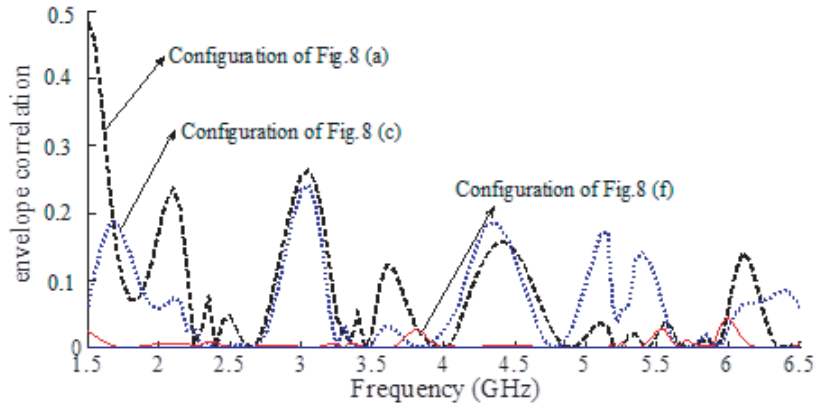


Figure 9. Simulated envelope correlation of the MIMO configured structures of Figs. 9(a), (c) and (f).

Based on the fact that an array of orthogonal elements results in low mutual coupling and envelope correlation and also as the capacity of the channel increases with polarization and pattern diversity [2], Fig. 7(f) is the most suitable for MIMO applications.

It should be mentioned that the dimension of the antenna given earlier is for single element. Once placed in an array configuration, due to coupling between elements, slight shifts in centre frequency of resonances takes place. To obtain the resonances at desired frequencies, the following dimensions for array elements are used. Optimized dimensions of antenna 1 are $Ls1 = 16.2$ mm, $Ls2 = 16.7$ mm, $Ls3 = 16.55$ mm and $Ls4 = 11.15$ mm, and dimensions of antenna 2 are $Ls1 = 16.15$ mm, $Ls2 = 16.55$ mm, $Ls3 = 16.55$ mm and $Ls4 = 11.25$ mm.

The simulated envelope correlation of the array structure of Fig. 7(f) is shown in Fig. 9, and the envelope correlation in the all bands is less than 0.02.

Figure 8(f) shows the measured S -parameters of the antenna array structure of Fig. 7(f). The measured impedance bandwidth meets the required bandwidth specification for UMTS, WLAN and WiMAX operation with reflection coefficient below -10 dB. For the isolation between the array elements,

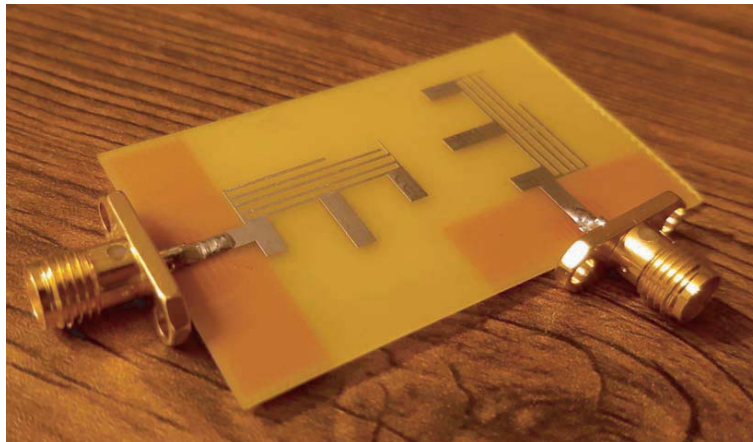


Figure 10. Fabricated Proposed MIMO antenna.

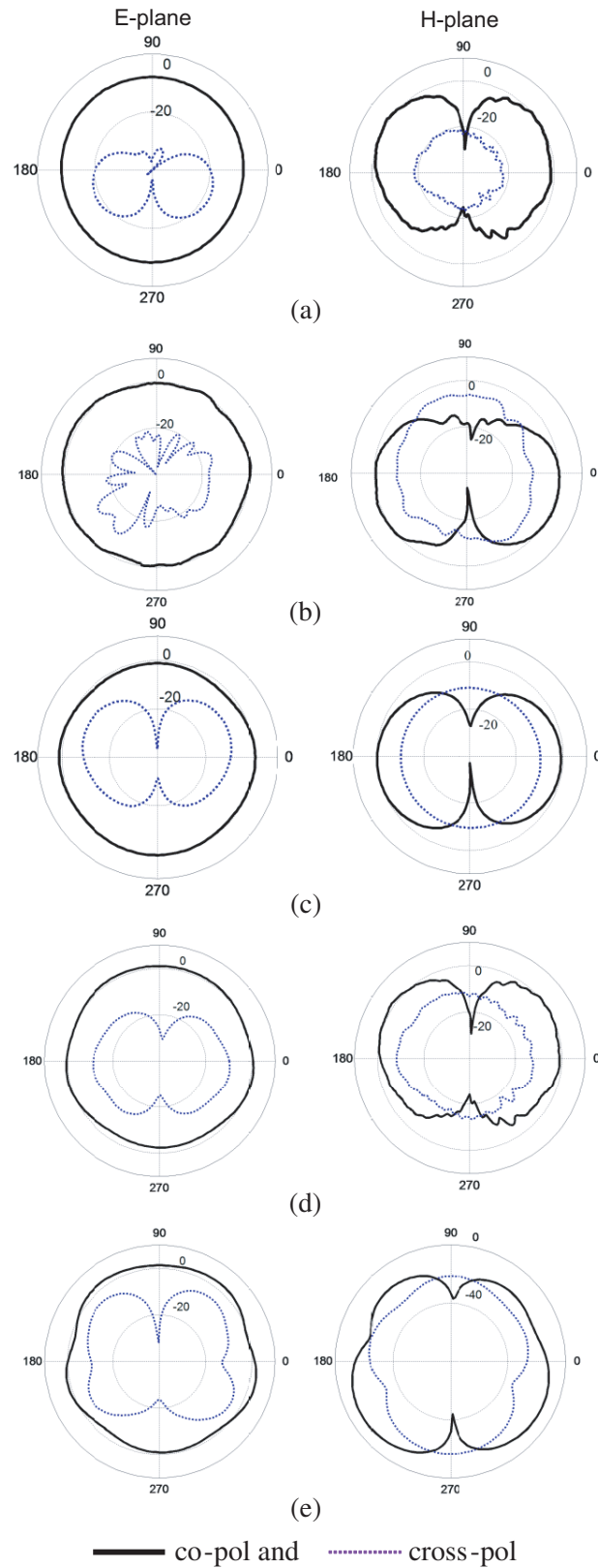


Figure 11. *E*- and *H*-plane radiation patterns of the proposed MIMO configured E-shaped antenna of structure shown in Fig. 7(f), at (a) 2.1 GHz, (b) 2.5 GHz, (c) 3.5 GHz, (d) 5.2 GHz, (e) 5.8 GHz.

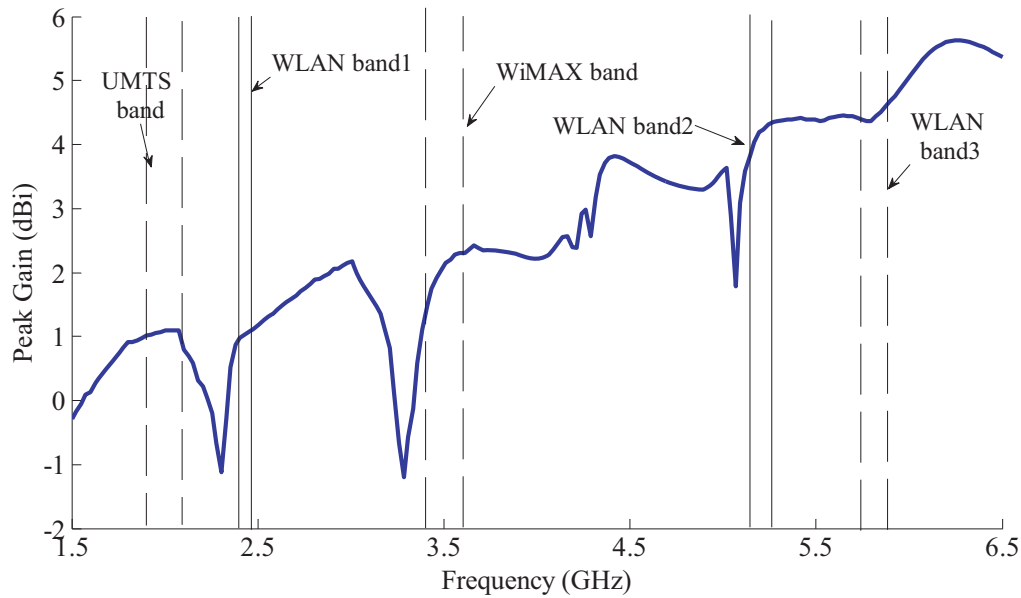


Figure 12. Measured peak gain of the proposed MIMO configured E-shaped antenna of structure shown in Fig. 7(f).

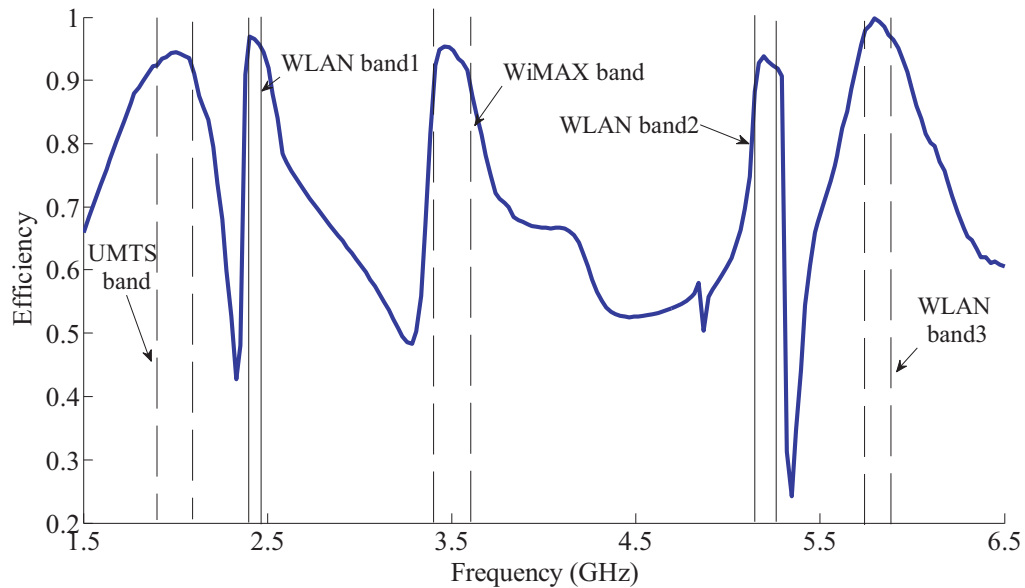


Figure 13. Measured radiation efficiency of the proposed MIMO configured E-shaped antenna of structure shown in Fig. 7(f).

it is found below -14 dB for 5.8 GHz and -20 dB for other frequencies.

The fabricated proposed antenna is shown in Fig. 10. The measured E -plane and H -plane co- and cross-polarization radiation patterns at 2.1, 2.5, 3.5, 5.2 and 5.8 GHz are shown in Fig. 11. It is noticed that the E -plane pattern is omnidirectional and has lower than -10 dB cross polarization over all the frequency bands. Also, the H -plane pattern is very stable with changes in frequency. Fig. 12 shows the simulated peak gain of the MIMO antenna. The peak gain over the WLAN range varies from 1 to 6 dB.

Simulated radiation efficiency is shown in Fig. 13. The radiation efficiency is obtained by calculating the ratio of the total radiated power of the array antenna to the total input power. For all frequency

bands of interest, the radiation efficiency is between 94 and 99.5%.

The low mutual coupling shown in Fig. 8(f), the low envelope correlation shown in Fig. 9 and the good omnidirectional radiation patterns shown in Fig. 10 confirm that the proposed antenna array structure of Fig. 7(f) is a good candidate for use in multi-band MIMO applications.

6. CONCLUSION

A penta-band E-shaped printed monopole antenna loaded with narrow slots and stubs suitable for MIMO application has been presented. The antenna parameters for UMTS, WLAN and WiMAX application, covering the 2.1, 2.5, 3.5, 5.2 and 5.8 GHz are given. Six array configurations of such two antennas for MIMO application are compared. The proposed MIMO array configuration with element spacing of $\lambda_g/15$ provides less than -14 dB mutual coupling, envelope correlation of lower than 0.02, average peak gain of 2.5 dBi, efficiency of higher than 94% and stable omnidirectional patterns over all five frequencies. Orthogonal array configuration is simple, low cost and easy fabrication idea for obtained good results in MIMO antenna.

REFERENCES

1. Vaughan, R. G. and J. B. Andersen, "Antenna diversity in mobile communication," *IEEE Trans. Vehicular Technol.*, Vol. 36, 149–172, 1987.
2. Forenza, A. and R. W. Heath, "Benefit of pattern diversity via two element array of circular patch antennas in indoor clustered MIMO channels," *IEEE Trans. Commun.*, Vol. 54, 943–954, 2006.
3. Mohammad-Ali-Nezhad, S., H. R. Hassani, and A. Foudazi, "A dual-band WLAN/UWB printed wide slot antenna for mimo/diversity applications," *Microwave Opt. Technol. Lett.*, Vol. 55, 461–465, 2013.
4. Mallahzadeh, A. R., S. F. Seyyedrezaei, N. Ghahvehchian, S. Mohammad-Ali-Nezhad, and S. Mallahzadeh, "Tri-band printed monopole antenna for WLAN and WiMAX MIMO systems," *5th European Conference on Antennas and Propagation (EUCAP)*, 548–551, 2011.
5. Yang, L., H. Xu, J. Fang, and T. Li, "Four-element dual-band MIMO antenna system for mobile phones," *Progress In Electromagnetics Research C*, Vol. 60, 47–56, 2015.
6. Khan, A. A., M. H. Jamaluddin, J. Nair, R. Khan, S. Aqeel, J. Saleem and Owais, "Design of a dual-band MIMO dielectric resonator antenna with pattern diversity for WiMAX and WLAN applications," *Progress In Electromagnetics Research M*, Vol. 50, 65–73, 2016.
7. Chen, S. and K.-M. Luk, "A dual-mode wideband MIMO cube antenna with magneto-electric dipoles," *IEEE Trans. Antennas Propag.*, Vol. 62, 5951–5959, 2014.
8. Kumar, N. and U. K. Kommuri, "MIMO antenna mutual coupling reduction for WLAN using spiro meander line UC-EBG," *Progress In Electromagnetics Research C*, Vol. 80, 65–77, 2018.
9. Pan, B. C. and T. J. Cui, "Broadband decoupling network for dual-band microstrip patch antennas," *IEEE Trans. Antennas Propag.*, Vol. 65, 5595–5598, 2017.
10. Arya, A. K., N. V. Anh, R. S. Aziz, B. Y. Park, and S. O. Park, "Dual polarized dual antennas for 1.7–2.1 GHz LTE base stations," *IEEE Antennas Wireless Propag. Lett.*, Vol. 14, 1427–1430, 2015.
11. Zhao, L., L. Liu, and Y.-M. Cai, "A MIMO antenna decoupling network composed of inverters and coupled split ring resonators," *Progress In Electromagnetics Research C*, Vol. 79, 175–183, 2017.
12. Liu, P., D. Sun, P. Wang, and P. Gao, "Design of a dual-band MIMO antenna with high isolation for WLAN applications," *Progress In Electromagnetics Research Letters*, Vol. 74, 23–30, 2018.
13. Mohammad-Ali-Nezhad, S. and H. R. Hassani, "A novel tri-band E-shaped printed monopole antenna for MIMO application," *IEEE Antennas Wireless Propag. Lett.*, Vol. 9, 576–579, 2010.
14. Foudazi, A., A. R. Mallahzadeh, and S. Mohammad-Ali-Nezhad, "A triple-band WLAN/WiMAX printed monopole antenna for MIMO applications," *Microw. Opt. Technol. Lett.*, Vol. 54, 1321–1325, 2012.
15. Fang, Q., D. Mi, and Y. Yin, "A tri-band MIMO antenna for WLAN/WiMAX application," *Progress In Electromagnetics Research Letters*, Vol. 55, 75–80, 2015.

16. Karimian, R., H. Oraizi, S. Fakhte, and M. Farahani, "Novel F-shaped quad-band printed slot antenna for WLAN and WiMAX MIMO systems," *IEEE Antennas Wireless Propag. Lett.*, Vol. 12, 405–408, 2013.
17. Sarkar, D., A. Singh, K. Saurav, and K. V. Srivastava, "Four-element quad-band multiple-input-multiple-output antenna employing split-ring resonator and inter-digital capacitor," *IET Microw. Antennas Propag.*, Vol. 9, 1453–1460, 2015.
18. Sharawi, M. S., "Current misuses and future prospects for printed multiple-input, multiple-output antenna systems," *IEEE Antennas Propag. Mag.*, Vol. 59, 162–170, 2017.